

# Solutions of Differential–Difference Equations Arising from Mathematical Models of Granulocytopoiesis

Mani Mehra · Ranjan K. Mallik

Published online: 3 February 2013

© Foundation for Scientific Research and Technological Innovation 2013

**Abstract** The closed form solutions of differential–difference equations arising from mathematical models of granulocytopoiesis, both with and without maturing cells, are presented. The model with maturing cells, which we call model I, is considered first. The solution technique consists of a Laplace transform approach that converts each of the two differential–difference equations to a difference equation in the transform domain, and subsequent Laplace transform inversion of the solution to express it in the time domain. The model without maturing cells, which we call model II, is next considered and is solved by a method similar to that for model I. From these solutions, useful information and properties, like average number of active and maturing cells, and the transient growth and half-life periods of cells in each stage, can be obtained analytically. This information can play a very crucial role in the treatment of granulocytopoiesis. Further, the numerical solution of another model, which we call model III, for describing the dynamics of imatinib (drug used to treat certain types of cancer)-treated chronic myelogenous leukemia is discussed using a wavelet adaptive computational approach.

**Keywords** Closed form solution · Differential–difference equation · Granulocytopoiesis · Laplace transform · Wavelets

## Introduction

Granulocytopoiesis or granulopoiesis (production of white blood cells) is hematopoiesis (formation of blood cellular components) of granulocytes (category of white blood cells)

---

M. Mehra (✉)

Department of Mathematics, Indian Institute of Technology Delhi, Hauz Khas, New Delhi 110016, India  
e-mail: mmehra@maths.iitd.ac.in

R. K. Mallik

Department of Electrical Engineering, Indian Institute of Technology Delhi,  
Hauz Khas, New Delhi 110016, India  
e-mail: rkmallik@ee.iitd.ernet.in

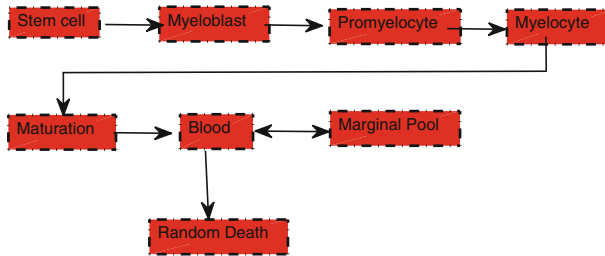


**Fig. 1** Process of granulocytopoiesis

beginning with stem cells (a cell that has the potential to regenerate tissue over a lifetime). It occurs mainly within the bone marrow. The process is illustrated in Fig. 1, where myeloblasts, promyelocytes, and myelocytes are *proliferative* cells. The maturation block consists of metamyelocytes, band forms, and granulocytes, all of which *nonproliferative*. The proliferative cells go through a number of stages either by dividing a certain number of times or by maturing without further dividing. For each cell type, there is a specific number  $n$  of stages, a certain time that a cell remains in each stage, and a number  $f$  (fraction of cells that continues dividing as opposed to maturing). In the mathematical model of granulocytopoiesis, myeloblasts go through 3 stages ( $n_b = 3$ ), promyelocytes go through 2 stages ( $n_p = 2$ ), and myelocytes go through 1 stage ( $n_m = 1$ ), where  $n_b$ ,  $n_p$ , and  $n_m$  denote the respective number of stages. However, nonproliferative cells have one stage only.

We now turn to the kinetics of the process of granulocytopoiesis. The transit time from stem cell to myelocyte (the proliferative block) is in the vicinity of 140h under normal conditions [1]. Movement of granulocytes through the maturation block is believed to be a “first in, first out” process in [2]. This information is derived from experimental measurements and computer simulation of the process of granulocytopoiesis, which are prone to have some errors. This information of cell kinetics has proved to be the key to predicting some type of control mechanism for granulocytopoiesis. Our objective here is to provide a mechanism for obtaining the same sort of information without errors. Closed form solutions of differential–difference equations governing these processes, that serve as an effective tool for providing information such as average number of active and maturing cells, and the transient growth and half-life periods of cells in each stage, are derived in this paper. Another model which leads to difference equations is described in [3,4].

The mathematical model of granulocytopoiesis considered in [5] describes both the normal process and the chronic myelogenous leukemia (CML) with different parameters values. It is more complete than the previously defined models [6–8]. CML, also known as chronic granulocyte leukemia (CGL), is a cancer of white blood cells [9] and represents 20% of all leukemias. It is a form of leukemia characterized by the increased and unregulated growth of myeloid cells in the bone marrow and accumulation of these cells in the blood. CML is a clonal bone marrow stem cell disorder in which proliferation of mature granulocytes and their precursors is the main finding. CML is often suspected on the basis on the complete blood count, which shows increased granulocytes of all types. The recently developed drug imatinib has proven to be a highly effective and first-line treatment for CML by Druker and Lydon [10] compared to the previous standard treatment of chemotherapy or stem cell transplantation by Campbell et al. [11].

In recent years, there has been many more works deriving mathematical models of CML and related to that. Some of them are as follows. A simulation study of cyclical granulopoiesis in chronic granulocytic leukemia is given in [12]. The model of neutrophil production is

simulated numerically by Rubinow and Lebowitz [8] due to lack of analytical solution and its steady state behavior is demonstrated. The model of stem cell proliferation is developed by Loeffler and Wichmann [13]. A model that accounts for the immune response in CML is presented in [14]. The aim of the work presented in [15] is to identify the parameters that control cancer remission. In [16], a model describing the dynamics of imatinib treated CML is presented as a system of difference equations, and its continuous extension is presented as a system of partial differential equations in [17]. All these works have been motivated by the hope to control cancer in a significant manner. However, these works have not been able to characterize analytically the transient behavior of cell growth. Motivated by this fact, we analyze the transient behavior of cell growth in our work, using the mathematical model of granulocytopoiesis presented in [5], which is the most comprehensive model available till date to the best of our knowledge.

In the later part of this paper, the numerical solution of the model described in [17] is discussed using an adaptive computational approach. Wavelet methods for simulating partial differential equations (PDEs) compose a relatively new research field and have been already proved as efficient tools for simulating PDEs [18–20] whose solutions require locally adapted grid. In recent years, wavelet analysis has been applied to a large variety of biomedical signals [21]. The ability of wavelets to identify and isolate localized structures has made them attractive candidates for adaptive computation. Here we solve PDEs using a wavelet adaptive computational approach. This is the first attempt, to the best of our knowledge, where this approach has been applied to PDEs arising from cancer modelling.

In this paper, we derive closed form solutions of the differential–difference equations arising from mathematical models of granulocytopoiesis considered in [5], both with and without maturing cells. The model with maturing cells (that is, involving both active and maturing cells), which we call model I, is considered first. The solution technique consists of a Laplace transform approach that converts each of the two differential–difference equations to a difference equation in the transform domain, and subsequent Laplace transform inversion of the solution to express it in the time domain. The model without maturing cells (that is, involving active cells only), which we call model II, is next considered and is solved by a method similar to that for model I. Note that the limitation of the analytical method used is linearity of the differential–difference equation which governs a particular model. The numerical aspects of another model [17], which we call model III, are also discussed.

### Mathematical Model of Granulocytopoiesis With Maturing Cells (Model I)

#### Formulation of Model I

Some symbols used in formulating the mathematical model of granulocytopoiesis are shown in Table 1. Note from Fig. 1 that a stem cell passes through a succession of stages before it

**Table 1** Symbols used in formulating the mathematical model of granulocytopoiesis

$f_b, f_p, f_m$	Fractions of myeloblasts, promyelocytes, myelocytes, respectively, which will continue dividing
$n_b, n_p, n_m$	Number of stages of myeloblasts, promyelocytes, myelocytes, respectively
$A_0$ ( $\text{kg}^{-1}$ )	Total number of active stem cells
$q$ ( $\text{h}^{-1}\text{kg}^{-1}$ ) = $\frac{2A_0}{T_0}$	Rate at which myeloblasts are produced by stem cells

reaches the blood stream. Stem cells produce myeloblasts in stage 1 at the rate of  $q$  cells per unit time per kilogram of body weight, where  $q = (2A_0)/T_0$  (see Table 1). A fraction  $f_1$  of these cells is active. After a time  $T_1$ , the active cells divide remaining myeloblasts while the rest of the cells enter stage 2 by maturing. After  $n_b$  such stages or equivalent maturation, the myeloblasts becomes promyelocytes. After  $n_p$  further stages or equivalent maturation the promyelocytes become myelocytes, and after  $n_m$  more stages or equivalent maturation myelocytes enter the maturation block and finally enter into the blood. Using the notations in Table 1, the mathematical model of granulocytopoiesis with maturing cells, as considered in [5], is given by

$$T_j \frac{dA_j}{dt} = -A_j + 2f_j \frac{T_j}{T_{j-1}} A_{j-1},$$

$$j = 1, 2, \dots, n_b + n_p + n_m, \tag{2.1a}$$

$$T_j \frac{dM_j}{dt} = -M_j + 2(1 - f_j) \frac{T_j}{T_{j-1}} A_{j-1} + \frac{T_j}{T_{j-1}} M_{j-1},$$

$$j = 1, 2, \dots, n_b + n_p + n_m, \tag{2.1b}$$

where  $A_j(t)$  (in short form  $A_j$ ) denotes the *number of active cells* in stage  $j$  at time  $t$  and  $M_j(t)$  (in short form  $M_j$ ) denotes the *number of maturing cells* in stage  $j$  at time  $t$ , with  $M_0(t) = 0$ . Note that (2.1a) and (2.1b) are differential–difference equations in  $A_j(t)$  and  $M_j(t)$ , respectively.

### Closed Form Solution of Model I

By using the explicit solutions of linear difference equations presented in [22,23], we solve Eqs. (2.1a) and (2.1b) in closed form.

We use the Laplace transform approach to convert these equations to difference equations. Let  $A_j(0)$  and  $M_j(0)$  be the initial values of  $A_j(t)$  and  $M_j(t)$ , respectively, at time  $t = 0$ , and let  $\mathbf{A}_j(s)$  and  $\mathbf{M}_j(s)$  denote, respectively, their one-sided Laplace transforms, given by

$$\mathbf{A}_j(s) = \int_0^\infty A_j(t) \exp(-st)dt, \quad \mathbf{M}_j(s) = \int_0^\infty M_j(t) \exp(-st)dt. \tag{2.2}$$

Consider now the differential–difference equation (2.1a). Taking Laplace transforms of both sides, we get

$$T_j \left( s\mathbf{A}_j(s) - A_j(0) \right) = -\mathbf{A}_j(s) + 2f_j \frac{T_j}{T_{j-1}} \mathbf{A}_{j-1}(s), \tag{2.3}$$

which results in the first-order linear difference equation (in the index  $j$ )

$$\mathbf{A}_j(s) = \frac{2f_j T_j}{T_{j-1}(sT_j + 1)} \mathbf{A}_{j-1}(s) + \frac{T_j}{(sT_j + 1)} A_j(0), \tag{2.4}$$

with initial condition  $\mathbf{A}_0(s)$ . This can be expressed in the form

$$\mathbf{A}_j(s) = \alpha_j \mathbf{A}_{j-1}(s) + \beta_j, \tag{2.5}$$

where

$$\alpha_j = \frac{2f_j T_j}{T_{j-1}(sT_j + 1)}, \quad \beta_j = \frac{T_j}{(sT_j + 1)} A_j(0). \tag{2.6}$$

The solution of (2.5) is given by [22]

$$A_j(s) = \left[ \prod_{i=1}^j \alpha_i \right] A_0(s) + \sum_{k=1}^{j-1} \left[ \prod_{i=k+1}^j \alpha_i \right] \beta_k + \beta_j. \tag{2.7}$$

Substituting (2.6) in (2.7), we get

$$A_j(s) = \frac{\left[ \prod_{i=1}^j \frac{2f_i T_i}{T_{i-1}} \right]}{\prod_{i=1}^j (sT_i + 1)} A_0(s) + \sum_{k=1}^{j-1} \frac{\left[ \prod_{i=k+1}^j \frac{2f_i T_i}{T_{i-1}} \right] T_k A_k(0)}{\prod_{i=k}^j (sT_i + 1)} + \frac{T_j A_j(0)}{(sT_j + 1)}. \tag{2.8}$$

To obtain the closed form solution for  $A_j(t)$  we need to do the Laplace inversion of  $A_j(s)$  in (2.8).

For distinct  $T_i$ 's, we can express, using partial fractions,

$$\frac{\prod_{i=k}^j T_i}{\prod_{i=k}^j (sT_i + 1)} = \sum_{l=k}^j \frac{c_{l,k,j}}{\left( s + \frac{1}{T_l} \right)}, \tag{2.9a}$$

where

$$c_{l,k,j} = \frac{1}{\prod_{\substack{m=k \\ m \neq l}}^j \left( \frac{1}{T_m} - \frac{1}{T_l} \right)}. \tag{2.9b}$$

Taking inverse Laplace transform, we get

$$\mathcal{L}^{-1} \left\{ \sum_{l=k}^j \frac{c_{l,k,j}}{\left( s + \frac{1}{T_l} \right)} \right\} = \sum_{l=k}^j c_{l,k,j} \exp\left(-\frac{t}{T_l}\right) u(t), \tag{2.10}$$

where  $u(\cdot)$  denotes the unit step function. Further, we have

$$\mathcal{L}^{-1} \left\{ \frac{1}{\left( s + \frac{1}{T_l} \right)} A_0(s) \right\} = \exp\left(-\frac{t}{T_l}\right) u(t) * A_0(t) = \int_0^t \exp\left(-\frac{(t-\tau)}{T_l}\right) A_0(\tau) d\tau, \tag{2.11}$$

where  $*$  denotes convolution. Substituting (2.9) in (2.8) and taking the inverse Laplace transform using (2.10) and (2.11), we can express  $A_j(t)$  as

$$\begin{aligned} A_j(t) &= \left[ \prod_{i=1}^j \frac{2f_i}{T_{i-1}} \right] \sum_{l=1}^j c_{l,1,j} \int_0^t \exp\left(-\frac{(t-\tau)}{T_l}\right) A_0(\tau) d\tau \\ &+ \sum_{k=1}^{j-1} \left[ \prod_{i=k+1}^j \frac{2f_i}{T_{i-1}} \right] A_k(0) \sum_{l=k}^j c_{l,k,j} \exp\left(-\frac{t}{T_l}\right) u(t) \\ &+ A_j(0) \exp\left(-\frac{t}{T_j}\right) u(t). \end{aligned} \tag{2.12}$$

Since  $A_j(t)$  has support  $[0, T_j)$ , an expression for  $A_j(t)$  in closed form (in terms of  $A_0(t)$ ) is obtained from (2.12) as

$$\begin{aligned}
 A_j(t) = & \left[ \prod_{i=1}^j \frac{2f_i}{T_{i-1}} \right] \sum_{l=1}^j c_{l,1,j} \int_0^{\min(t, T_0)} \exp\left[-\frac{(t-\tau)}{T_l}\right] A_0(\tau) d\tau \\
 & + \sum_{k=1}^{j-1} \left[ \prod_{i=k+1}^j \frac{2f_i}{T_{i-1}} \right] A_k(0) \sum_{l=k}^j c_{l,k,j} \exp\left(-\frac{t}{T_l}\right) \\
 & + A_j(0) \exp\left(-\frac{t}{T_j}\right), \quad 0 \leq t < T_j.
 \end{aligned}
 \tag{2.13}$$

Next we consider the differential–difference equation (2.1b). Laplace transformation of both sides results in the first-order linear difference equation (in the index  $j$ )

$$\mathbf{M}_j(s) = \frac{T_j}{T_{j-1}(sT_j + 1)} \mathbf{M}_{j-1}(s) + \frac{T_j M_j(0) + \frac{2(1-f_j)T_j}{T_{j-1}} \mathbf{A}_{j-1}(s)}{(sT_j + 1)}, \tag{2.14}$$

with initial condition  $\mathbf{M}_0(s)$ . Equation (2.14) has the same structure as (2.5). Solving (2.14) in the same way as (2.5) gives rise to

$$\begin{aligned}
 \mathbf{M}_j(s) = & \frac{\left[ \prod_{i=1}^j \frac{T_j}{T_{i-1}} \right]}{\prod_{i=1}^j (sT_i + 1)} \mathbf{M}_0(s) \\
 & + \sum_{k=1}^{j-1} \frac{\left[ \prod_{i=k+1}^j \frac{T_i}{T_{i-1}} \right] \left\{ T_k M_k(0) + \frac{2(1-f_k)T_k}{T_{k-1}} \mathbf{A}_{k-1}(s) \right\}}{\prod_{i=k}^j (sT_i + 1)} \\
 & + \frac{T_j M_j(0) + \frac{2(1-f_j)T_j}{T_{j-1}} \mathbf{A}_{j-1}(s)}{(sT_j + 1)}.
 \end{aligned}
 \tag{2.15}$$

Applying (2.9) and taking the inverse Laplace transform of (2.15) using (2.10) and (2.11), we can express  $M_j(t)$  as

$$\begin{aligned}
 M_j(t) = & \left[ \prod_{i=1}^j \frac{1}{T_{i-1}} \right] \sum_{l=1}^j c_{l,1,j} \int_0^t \exp\left(-\frac{(t-\tau)}{T_l}\right) M_0(\tau) d\tau \\
 & + \sum_{k=1}^{j-1} \left[ \prod_{i=k+1}^j \frac{1}{T_{i-1}} \right] \sum_{l=k}^j c_{l,k,j} \left\{ M_k(0) \exp\left(-\frac{t}{T_l}\right) u(t) \right. \\
 & \left. + \frac{2(1-f_k)}{T_{k-1}} \int_0^t \exp\left(-\frac{(t-\tau)}{T_l}\right) A_{k-1}(\tau) d\tau \right\} \\
 & + \left\{ M_j(0) \exp\left(-\frac{t}{T_j}\right) u(t) + \frac{2(1-f_j)}{T_{j-1}} \int_0^t \exp\left(-\frac{(t-\tau)}{T_j}\right) A_{j-1}(\tau) d\tau \right\}.
 \end{aligned}
 \tag{2.16}$$

Since  $A_j(t)$  and  $M_j(t)$  have support  $[0, T_j)$ , we obtain from (2.16) an expression for  $M_j(t)$  in closed form (in terms of  $M_0(t)$  and  $A_0(t), \dots, A_{j-1}(t)$ ), which is given by

$$\begin{aligned}
 M_j(t) = & \left[ \prod_{i=1}^j \frac{1}{T_{i-1}} \right] \sum_{l=1}^j c_{l,1,j} \int_0^{\min(t, T_0)} \exp\left(-\frac{(t-\tau)}{T_l}\right) M_0(\tau) d\tau \\
 & + \sum_{k=1}^{j-1} \left[ \prod_{i=k+1}^j \frac{1}{T_{i-1}} \right] \sum_{l=k}^j c_{l,k,j} \left\{ M_k(0) \exp\left(-\frac{t}{T_l}\right) \right. \\
 & \left. + \frac{2(1-f_k)}{T_{k-1}} \int_0^{\min(t, T_{k-1})} \exp\left[-\frac{(t-\tau)}{T_l}\right] A_{k-1}(\tau) d\tau \right\} \\
 & + \left\{ M_j(0) \exp\left(-\frac{t}{T_j}\right) + \frac{2(1-f_j)}{T_{j-1}} \int_0^{\min(t, T_{j-1})} \exp\left(-\frac{(t-\tau)}{T_j}\right) A_{j-1}(\tau) d\tau \right\}, \\
 & 0 \leq t < T_j, \tag{2.17}
 \end{aligned}$$

where  $A_j(t)$  is given in closed form by (2.13).

In Eqs. (2.1a) and (2.1b), we do not make any distinction with respect to different cells and consider the total number of stages as  $n_b + n_p + n_m$ . However, to explain the steady state version of the model, we distinguish the parameters with respect to different cells. Equations (2.1a) and (2.1b) admit steady state solutions  $A_j^b$  and  $M_j^b$  ( $A_j^b = A_j$ ,  $M_j^b = M_j$ ,  $1 \leq j \leq n_b$ ) in case of myeloblasts,  $A_j^p$  and  $M_j^p$  ( $A_j^p = A_{n_b+j}$ ,  $M_j^p = M_{n_b+j}$ ,  $1 \leq j \leq n_p$ ) in case of promyelocytes,  $A_j^m$  and  $M_j^m$  ( $A_j^m = A_{n_b+n_p+j}$ ,  $M_j^m = M_{n_b+n_p+j}$ ,  $1 \leq j \leq n_m$ ) in case of myelocytes, which are given by [5]

$$\begin{aligned}
 \frac{A_j^b}{T_b} &= (2f_b)^j \frac{A_0}{T_0}, \quad j = 1, 2, \dots, n_b, \\
 \frac{A_j^p}{T_p} &= (2f_p)^j \frac{A_{n_b}^b}{T_b}, \quad j = 1, 2, \dots, n_p, \\
 \frac{A_j^m}{T_m} &= (2f_m)^j \frac{A_{n_p}^p}{T_p}, \quad j = 1, 2, \dots, n_m, \tag{2.18a}
 \end{aligned}$$

$$\begin{aligned}
 \frac{M_j^b}{T_b} &= a_{bj} \frac{A_0}{T_0}, \quad j = 1, 2, \dots, n_b, \\
 \frac{M_j^p}{T_p} &= a_{pj} \frac{A_{n_b}^b}{T_b} + \frac{M_{n_b}^b}{T_b}, \quad j = 1, 2, \dots, n_p, \\
 \frac{M_j^m}{T_m} &= a_{mj} \frac{A_{n_p}^p}{T_p} + \frac{M_{n_p}^p}{T_p}, \quad j = 1, 2, \dots, n_m, \tag{2.18b}
 \end{aligned}$$

where

$$\begin{aligned}
 T_b &= T_j, \quad f_b = f_j, \quad j = 1, \dots, n_b, \\
 T_p &= T_{n_b+j}, \quad f_p = f_{n_b+j}, \quad j = 1, \dots, n_p, \\
 T_m &= T_{n_b+n_p+j}, \quad f_p = f_{n_b+n_p+j}, \quad j = 1, \dots, n_m,
 \end{aligned}$$

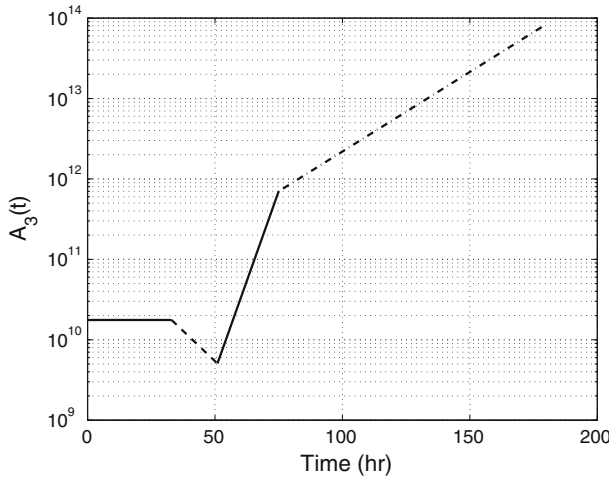


**Fig. 2** Number of cells

$$a_{bj} = 2(1 - f_b) \left( \frac{(2f_b)^j - 1}{2f_b - 1} \right), \quad a_{pj} = 2(1 - f_p) \left( \frac{(2f_p)^j - 1}{2f_p - 1} \right),$$

$$a_{mj} = 2(1 - f_m) \left( \frac{(2f_m)^j - 1}{2f_m - 1} \right).$$

The fit of some experimental data to the steady state model (2.18) has been shown in [5].

Significance of the Closed Form Solution of Model I Discussed in Previous Subsection

The closed form solution of the original model characterizing the transient behavior of granulocytopoiesis with maturing cells is given by (2.12) and (2.16). From the analytical expressions of  $A_j(t)$  in (2.12) and  $M_j(t)$  in (2.16), we can obtain many meaningful quantities. For example, the average number of active and maturing cells ( $\bar{A}_j$  and  $\bar{M}_j$ ) in each stage  $j$  can be computed as

$$\bar{A}_j = \frac{1}{T_j} \int_0^{T_j} A_j(t) dt, \quad \bar{M}_j = \frac{1}{T_j} \int_0^{T_j} M_j(t) dt.$$

In particular, the average number of active promyelocytes in the  $j$ th promyelocyte stage ( $\bar{A}_j^p$ ), which corresponds to the overall  $(n_b + j)$ th stage, can be computed as

$$\bar{A}_j^p = \frac{1}{T_p} \int_0^{T_{n_b+j}} A_{n_b+j}(t) dt.$$

We take the initial values from [24] as  $A_0(0) = 1.768 \times 10^{10}$ ,  $A_1(0) = 0.54 \times 10^{10}$ ,  $A_2(0) = 1.44 \times 10^{10}$ ,  $A_3(0) = 18.7 \times 10^{10}$  and let  $f_1 = 0.8$ ,  $f_2 = 0.6$ , and  $f_3 = 0.5$ ,  $T_0 = 33$  h,  $T_1 = 18$  h,  $T_2 = 24$  h. The number of promyelocytes ( $A_3(t)$ ) at time  $t = 179$  h using the closed form solution (2.12) is plotted in Fig. 2. We observe from Fig. 2 that the number of myeloblasts decreases during the transit time  $T_1 = 18$  h. However, the numbers of promyelocytes and myelocytes increase, as expected. We can also calculate the half-life



of cells in a given stage from these expressions. For example, the half-life of active cells in stage  $j$ , which we denote as  $T_{H,A_j}$ , can be computed by solving the equation  $0.5A_j(0) = A_j(T_{H,A_j})$ . From (2.12), assuming  $A_0(t) = A_0$  (that is, a constant) in the 0th stage, this results in the equation

$$\begin{aligned}
 0.5A_j(0) = & A_0 \left[ \prod_{i=1}^j \frac{2f_i}{T_{i-1}} \right] \sum_{l=1}^j c_{l,1,j} T_l \exp\left(-\frac{T_{H,A_j}}{T_l}\right) \left\{ \exp\left(\frac{\min(T_{H,A_j}, T_0)}{T_l}\right) - 1 \right\} \\
 & + \sum_{k=1}^{j-1} \left[ \prod_{i=k+1}^j \frac{2f_i}{T_{i-1}} \right] A_k(0) \sum_{l=k}^j c_{l,k,j} \exp\left(-\frac{T_{H,A_j}}{T_l}\right) \\
 & + A_j(0) \exp\left(-\frac{T_{H,A_j}}{T_j}\right).
 \end{aligned} \tag{2.19}$$

which can be solved numerically to calculate the half-life  $T_{H,A_j}$  using appropriate choice of parameters. In particular, putting  $j = 1$  in (2.19), we can get the half-life of active cells in the first stage obtained by solving the equation

$$\begin{aligned}
 0.5A_1(0) = & A_0 \left[ \frac{2f_1}{T_0} \right] T_1 \exp\left(-\frac{T_{H,A_1}}{T_1}\right) \left\{ \exp\left(\frac{\min(T_{H,A_1}, T_0)}{T_1}\right) - 1 \right\} \\
 & + A_1(0) \exp\left(-\frac{T_{H,A_1}}{T_1}\right),
 \end{aligned} \tag{2.20}$$

which results in

$$\begin{aligned}
 T_{H,A_1} = & T_1 \ln \left[ \frac{1 - \frac{A_1(0)T_0}{2A_0f_1T_1}}{1 - \frac{A_1(0)T_0}{4A_0f_1T_1}} \right] \text{ if } T_{H,A_1} < T_0, \\
 = & T_1 \ln \left\{ \frac{4A_0f_1T_1}{A_1(0)T_0} \left[ \exp\left(\frac{T_0}{T_1}\right) - 1 \right] + 2 \right\} \text{ if } T_{H,A_1} > T_0.
 \end{aligned} \tag{2.21}$$

Moreover, we can predict the transient growth of active and maturing cells in each stage as well as globally, which can play very crucial role in the treatment of granulocytopenias.

### Mathematical Model of Granulocytopenias Without Maturing Cells (Model II)

#### Formulation of Model II

We now modify the model I discussed in the previous section by considering active cells only. The resting stem cells  $A_{-1}$  become active stem cells  $A_0$  after time  $T_{-1}$ . These active cells divide after a time  $T_0$  and a fraction  $1 - f$  of the cells return to the resting stage. The remaining fraction  $f$  of the cells proceed to stage 1. Cells in stage 1 divide after a time  $T_1$  and both types of cells proceed to stage 2. This procedure continues until cells reach stage  $m$ . Assuming that  $T_0 = T_1 = \dots = T_m$ , and denoting  $\kappa$  as

$$\kappa = \frac{T_0}{T_{-1}}, \tag{3.1}$$

we find that  $A_j(t)$  satisfies the differential–difference equations [5]

$$T_{-1} \frac{dA_{-1}}{dt} = -A_{-1} + 2(1 - f)\kappa^{-1}A_0, \tag{3.2a}$$

$$T_0 \frac{dA_0}{dt} = -A_0 + \kappa A_{-1}, \tag{3.2b}$$

$$T_0 \frac{dA_1}{dt} = -A_1 + 2fA_0, \tag{3.2c}$$

$$T_0 \frac{dA_j}{dt} = -A_j + 2A_{j-1}, \quad j = 2, \dots, m. \tag{3.2d}$$

Closed Form Solution of Model II

Taking Laplace transforms of both sides of (3.2a) and (3.2b), we get, in matrix form,

$$\begin{bmatrix} 1 + sT_{-1} & -2(1 - f)\kappa^{-1} \\ -\kappa & 1 + sT_0 \end{bmatrix} \begin{bmatrix} \mathbf{A}_{-1}(s) \\ \mathbf{A}_0(s) \end{bmatrix} = \begin{bmatrix} T_{-1}A_{-1}(0) \\ T_0A_0(0) \end{bmatrix}. \tag{3.3}$$

Solving (3.3) for  $\mathbf{A}_{-1}(s)$  and  $\mathbf{A}_0(s)$  using matrix inversion results in

$$\mathbf{A}_{-1}(s) = \frac{T_{-1} [A_{-1}(0) + 2(1 - f)A_0(0) + sT_0A_{-1}(0)]}{(2f - 1) + s(T_{-1} + T_0) + s^2T_{-1}T_0}, \tag{3.4a}$$

$$\mathbf{A}_0(s) = \frac{T_0 [A_{-1}(0) + A_0(0) + sT_{-1}A_0(0)]}{(2f - 1) + s(T_{-1} + T_0) + s^2T_{-1}T_0}. \tag{3.4b}$$

Next, we take the Laplace transform both sides of (3.2c) and solve for  $\mathbf{A}_1(s)$  to yield

$$\mathbf{A}_1(s) = \frac{T_0A_1(0) + 2f\mathbf{A}_0(s)}{(1 + sT_0)}. \tag{3.5}$$

Substituting (3.4b) in (3.5) gives

$$\mathbf{A}_1(s) = \frac{T_0 \begin{bmatrix} (2f - 1)A_1(0) + 2f(A_{-1}(0) + A_0(0)) \\ +s \{(T_{-1} + T_0)A_1(0) + 2fT_{-1}A_0(0)\} \\ +s^2T_{-1}T_0A_1(0) \end{bmatrix}}{(1 + sT_0) ((2f - 1) + s(T_{-1} + T_0) + s^2T_{-1}T_0)}. \tag{3.6}$$

Finally, taking the Laplace transform of both sides of (3.2d) results in the difference equation

$$\mathbf{A}_j(s) = \frac{2}{(sT_0 + 1)}\mathbf{A}_{j-1}(s) + \frac{T_0A_j(0)}{(sT_0 + 1)}, \tag{3.7}$$

with initial condition  $\mathbf{A}_1(s)$ . Solving (3.7) using the same approach as in Model I yields

$$\mathbf{A}_j(s) = \frac{2^{j-1}}{(sT_0 + 1)^{j-1}}\mathbf{A}_1(s) + T_0 \sum_{k=2}^j \frac{2^{j-k}A_k(0)}{(sT_0 + 1)^{j-k+1}}. \tag{3.8}$$

Taking the inverse Laplace transform of both sides of (3.8), we obtain

$$\begin{aligned}
 A_j(t) &= \frac{2^{j-1}}{(j-2)! T_0^{j-1}} \int_0^t \tau^{j-2} \exp\left(-\frac{\tau}{T_0}\right) A_1(t-\tau) d\tau \\
 &+ \sum_{k=2}^j \frac{2^{j-k} A_k(0)}{(j-k)! T_0^{j-k}} t^{j-k} \exp\left(-\frac{t}{T_0}\right) u(t).
 \end{aligned}
 \tag{3.9}$$

We can simplify (3.9) further using the structure of  $A_1(s)$  in (3.6), which can be expressed as

$$A_1(s) = \frac{C(s)}{\left(s + \frac{1}{T_0}\right) \left(s + \frac{1}{q_1}\right) \left(s + \frac{1}{q_2}\right)},
 \tag{3.10}$$

where

$$C(s) = \frac{\begin{bmatrix} (2f-1)A_1(0) + 2f(A_{-1}(0) + A_0(0)) \\ +s\{(T_{-1} + T_0)A_1(0) + 2fT_{-1}A_0(0)\} \\ +s^2T_{-1}T_0A_1(0) \end{bmatrix}}{T_{-1}T_0},
 \tag{3.11}$$

and  $-1/q_1, -1/q_2$  are the roots of the quadratic (in  $s$ ) equation

$$(2f-1) + s(T_{-1} + T_0) + s^2T_{-1}T_0 = 0,$$

which are given by

$$\begin{aligned}
 q_1 &= \frac{(T_{-1} + T_0) - \sqrt{(T_{-1} + T_0)^2 - 4T_{-1}T_0(2f-1)}}{2(2f-1)}, \\
 q_2 &= \frac{(T_{-1} + T_0) + \sqrt{(T_{-1} + T_0)^2 - 4T_{-1}T_0(2f-1)}}{2(2f-1)}.
 \end{aligned}
 \tag{3.12}$$

Using partial fractions,  $A_1(s)$  can be expressed as

$$A_1(s) = \frac{c_0}{\left(s + \frac{1}{T_0}\right)} + \frac{c_1}{\left(s + \frac{1}{q_1}\right)} + \frac{c_2}{\left(s + \frac{1}{q_2}\right)},
 \tag{3.13}$$

with

$$c_0 = \frac{C\left(-\frac{1}{T_0}\right)}{\left(\frac{1}{q_1} - \frac{1}{T_0}\right) \left(\frac{1}{q_2} - \frac{1}{T_0}\right)},
 \tag{3.14}$$

$$c_1 = \frac{C\left(-\frac{1}{q_1}\right)}{\left(\frac{1}{T_0} - \frac{1}{q_1}\right) \left(\frac{1}{q_2} - \frac{1}{q_1}\right)}, \quad c_2 = \frac{C\left(-\frac{1}{q_2}\right)}{\left(\frac{1}{T_0} - \frac{1}{q_2}\right) \left(\frac{1}{q_1} - \frac{1}{q_2}\right)},$$

where  $C(\cdot)$  is given by (3.11). Laplace inversion of (3.13) results in

$$A_1(t) = \left[ c_0 \exp\left(-\frac{t}{T_0}\right) + c_1 \exp\left(-\frac{t}{q_1}\right) + c_2 \exp\left(-\frac{t}{q_2}\right) \right] u(t).
 \tag{3.15}$$

Substituting (3.15) in (3.9), and using the result

$$\int x^j \exp(-x) dx = -j! \exp(-x) \sum_{k=0}^j \frac{x^k}{k!},$$

we get

$$\begin{aligned} A_j(t) &= \frac{2^{j-1} c_0}{(j-1)! T_0^{j-1}} \exp\left(-\frac{t}{T_0}\right) u(t) \\ &+ 2^{j-1} \sum_{i=1}^2 \frac{c_i q_i^{j-1}}{(q_i - T_0)^{j-1}} \left[ \exp\left(-\frac{t}{q_i}\right) - \exp\left(-\frac{t}{T_0}\right) \sum_{k=0}^{j-2} \frac{(q_i - T_0)^k}{k! T_0^k q_i^k} t^k \right] u(t) \\ &+ \sum_{k=0}^{j-2} \frac{2^k A_{j-k}(0)}{k! T_0^k} t^k \exp\left(-\frac{t}{T_0}\right) u(t). \end{aligned} \tag{3.16}$$

Since  $A_j(t)$  has support  $[0, T_0)$  in this case, we obtain from (3.16)  $A_j(t)$  in closed form as

$$\begin{aligned} A_j(t) &= \frac{2^{j-1} c_0}{(j-1)! T_0^{j-1}} \exp\left(-\frac{t}{T_0}\right) \\ &+ 2^{j-1} \sum_{i=1}^2 \frac{c_i q_i^{j-1}}{(q_i - T_0)^{j-1}} \left[ \exp\left(-\frac{t}{q_i}\right) - \exp\left(-\frac{t}{T_0}\right) \sum_{k=0}^{j-2} \frac{(q_i - T_0)^k}{k! T_0^k q_i^k} t^k \right] \\ &+ \sum_{k=0}^{j-2} \frac{2^k A_{j-k}(0)}{k! T_0^k} t^k \exp\left(-\frac{t}{T_0}\right), \quad 0 \leq t < T_0, \end{aligned} \tag{3.17}$$

where  $q_1, q_2$  are given by (3.12) and  $c_0, c_1, c_2$  by (3.14). The steady state version of the model (3.2) and fit of some experimental data are explained in [5].

### Significance of the Closed Form Solution of Model II Discussed in Previous Subsection

Again, we can predict useful transient information regarding this model from (3.16). For example, the half-life of active cells in the second stage, which we denote as  $T_{H,A_2}$ , can be obtained from the equation  $0.5A_2(0) = A_2(T_{H,A_2})$ , which [from (3.17)] is

$$\begin{aligned} 0.5A_2(0) &= \frac{2c_0}{T_0} \exp\left(-\frac{T_{H,A_2}}{T_0}\right) \\ &+ 2 \sum_{i=1}^2 \frac{c_i q_i}{(q_i - T_0)} \left[ \exp\left(-\frac{T_{H,A_2}}{q_i}\right) - \exp\left(-\frac{T_{H,A_2}}{T_0}\right) \right] \\ &+ A_2(0) \exp\left(-\frac{T_{H,A_2}}{T_0}\right). \end{aligned} \tag{3.18}$$

This can be solved numerically with appropriate choice of parameters to obtain  $T_{H,A_2}$ .

### Mathematical Model for Imatinib: Treated Chronic Myelogenous Leukemia

#### Formulation of Model III

In this model, the hematopoietic stem cells (HSCs) are assumed to exist in two growth compartments: Alpha (denoted by  $A$ ) and Omega (denoted by  $\Omega$ ). At the beginning of every time step (representing one hour), a stem cell may transfer from  $A$  to  $\Omega$  with probability  $\omega$  or from  $\Omega$  to  $A$  with probability  $\alpha$  as shown in Fig. 3, where the proliferating cells in the  $\Omega$  compartment progress through various stages of the cell cycle:  $G1$ ,  $S$ ,  $G2$  and  $M$ . The index of the stem cells is described by  $x = -\log a$ , where  $a$  is the affinity and  $x \in [x_{\min}, x_{\max}]$ . Let  $A(x, t)$  denote the population density of Alpha cells with  $x = \log a$  at time  $t$ . As time progresses, the  $x$ -components of these cells decrease at a constant rate until they reach  $x_{\min}$ . At this point, cells start accumulating at the boundary point  $x = x_{\min}$ . Let  $A^*(t)$  denote the population of Alpha cells at  $x = x_{\min}$  and  $\Omega(x, c, t)$  denote the population density of Omega cells with log affinity  $x$  and counter  $c$  at time  $t$ . As time progresses, the  $x$ -components of these cells increase at a constant rate until they reach  $x_{\max}$ . At the same time, the  $c$ -components (that record the position of the cells in their cell cycle) also increase at a constant rate. The cells that transfer into Omega from the  $A^*$  state enter at a point source  $P$  and travel along the appropriate characteristic curve with respect to  $x$  and  $c$ . Let  $\Omega^*(x, t)$  denote the population of cells that are transferred from  $A^*$  into the point source  $P$  at time  $t$ , and let  $\bar{A}$  and  $\bar{\Omega}$  denote the total population of cells in the  $A$  and  $\Omega$  compartments, respectively. Then

$$\bar{\Omega}(t) = \int_{x_{\min}}^{x_{\max}} \int_0^{49} \Omega(x, c, t) dc dx + \int_{x_{\min}}^{x_{\max}} \Omega^*(x, t) dx, \tag{4.1}$$

$$\bar{A}(t) = \int_{x_{\min}}^{x_{\max}} A(x, t) dx + A^*(t). \tag{4.2}$$

The points  $y_1, y_2, y_3, y_4$ , and  $y_5$  correspond to the  $x$ -values at which  $\Omega^*$  cells attain time counters of 49, 32, 49, 32, and 49, respectively, after entering the point source  $P$ . For details about the model one can refer to [17].

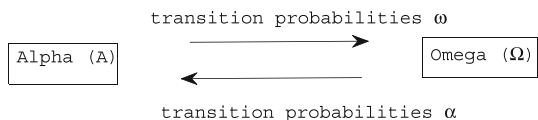
The formulation of the PDEs for each of the populations is as follows. For  $x \in [x_{\min}, x_{\max}]$ ,  $A$  satisfies

$$\begin{aligned} \frac{\partial A}{\partial t} - \rho_r \frac{\partial A}{\partial x} &= -\omega(\bar{\Omega}, \exp(-x))A + \alpha(\bar{A}, \exp(-x)) \int_0^{32} \Omega(x, c, t) dc \\ &+ \begin{cases} 0, & x \in X_a \\ -\alpha(\bar{A}, \exp(-x)), & x \in X_b, \end{cases} \end{aligned} \tag{4.3}$$

where

$$\begin{aligned} X_a &= (x_{\min}, y_1] \cup (y_2, y_3] \cup (y_4, y_5], \\ X_b &= (y_1, y_2] \cup (y_3, y_4] \cup (y_5, x_{\max}]. \end{aligned}$$

**Fig. 3** Transition probabilities of stem cell



Assuming that  $x_{\min} = 0$ , the values of  $y_i$  are given by  $y_1 = 17\rho_d$ ,  $y_2 = 49\rho_d$ ,  $y_3 = 66\rho_d$ ,  $y_4 = 98\rho_d$ ,  $y_5 = 115\rho_d$ , where the advection rate  $\rho_d$  is given by  $\log d$ , and  $d$  (differentiation factor)  $\approx 1.05$ . The left-hand side of the Eq. (4.3) accounts for the linear advection of the  $A$  population in the negative  $x$ -direction. The advection rate  $\rho_r$  is given by  $\log r$ , where  $r$  (regeneration factor) = 1.1 [25]. The first term on the right-hand side of the Eq. (4.3) accounts for the cells that transfer out of  $A$  into  $\Omega$ . The transition rate  $\omega$  is expressed as

$$\omega(\Omega(t), a(t)) = \frac{a_{\min}}{a(t)} f_w(\Omega(t)),$$

where  $\bar{\Omega}$  is given by Eq. (4.2) and  $f_w$  is the sigmoidal function. The second term on the right-hand side of Eq. (4.3) is the rate in which cells transfer into  $A$  from  $\Omega$ . The transition rate  $\alpha$  is expressed as

$$\alpha(A(t), a(t)) = \frac{a(t)}{a_{\max}} f_\alpha(\Omega(t)),$$

where  $\bar{A}$  is given by Eq. (4.1) and  $f_\alpha$  is the sigmoidal function. Only  $\Omega$  cells in the  $G1$  phase (i.e., with time counters  $c$  between 0 and 32) can transfer into  $A$ , which explains the boundaries in the integral. The last term on the right-hand side of Eq. (4.3) is the rate that cells transfer from  $\Omega^*$  into  $A$ . The quantity  $A^*$  is governed by the differential equation

$$\frac{dA^*}{dt} = -\omega(\bar{\Omega}, \exp(-x_{\min}))A^*(t) + \rho_r A(x_{\min}, t). \tag{4.4}$$

The PDE for  $\Omega$  is

$$\frac{\partial \Omega}{\partial t} + \rho_d \frac{\partial \Omega}{\partial x} + \frac{\partial \Omega}{\partial c} = \begin{cases} -\alpha(\bar{A}, \exp(-x)), & \text{for } c \in (0, 32] \\ 0, & \text{for } c \in (32, 49]. \end{cases} \tag{4.5}$$

Finally, the PDE for  $\Omega^*$  is

$$\frac{\partial \Omega^*}{\partial t} + \rho_d \frac{\partial \Omega^*}{\partial x} = \begin{cases} 0, & x \in X_a \\ -\alpha(\bar{A}, \exp(-x))\Omega^*, & x \in X_b. \end{cases} \tag{4.6}$$

Any cell in the  $\Omega$  compartment that has attained the maximal log affinity  $x_{\max}$  is destined to differentiate into a precursor cell. Hence, only cells with a smaller log affinity can exist in the  $A$  compartment, which means  $A(x_{\max}, t) = 0$ . Once  $\Omega$  cells reach the boundary  $c = 49$  they divide, and hence we have

$$\Omega(x, 0, t) = 2\Omega(x, 49, t).$$

At  $c = 32$ , we have  $\Omega(x, 32^+, t) = 2\Omega(x, 32^-, t) + w(\bar{\Omega}, \exp(-x))A$ . The boundary condition for  $\Omega^*$  at the point source  $P$  is

$$\Omega^*(x_{\min}, t) = \frac{\omega(\bar{\Omega}, \exp(-x_{\min}))}{\rho_d} A^*.$$

When the time counters  $c$  of the  $\Omega^*$  cells reach 49, i.e., at  $y_1, y_3$ , and  $y_5$ , cells divide, and hence we have

$$\Omega(y_i^+, t) = 2\Omega(y_i^+, t), \quad i = 1, 3, 5.$$

We also see that  $\Omega^*$  is continuous at  $y_2$  and  $y_4$ , and hence

$$\Omega(y_i^+) = \Omega(y_i^-, t), \quad i = 2, 4.$$

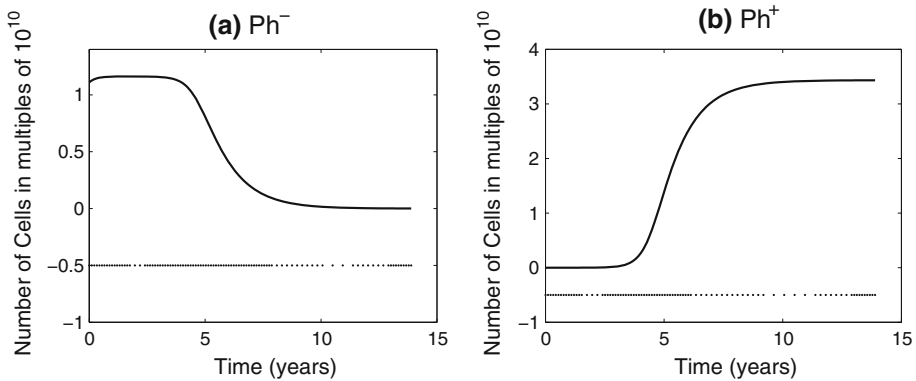


**Fig. 4** Numerical solution of PDE model ( $\text{Ph}^-$  and  $\text{Ph}^+$  cells)

The PDE for the precursor cells can thus be written as a linear advection equation that represents a simple age-based formulation, in the form

$$\frac{\partial P}{\partial t} + \frac{\partial P}{\partial s} = 0, \quad s \in [0, 480). \tag{4.7}$$

Similarly, the PDE for maturing cells is

$$\frac{\partial M}{\partial t} + \frac{\partial M}{\partial s} = 0, \quad s \in [0, 192), \tag{4.8}$$

where  $P(s, t)$  and  $M(s, t)$  denote the population density of precursor and maturing cells at stage  $s$  and time  $t$ , respectively. The PDEs for subpopulation  $\text{Ph}^-$  (nonleukemia cells) ( $A^-, A^{*-}, \Omega^-, \Omega^{*-}, P^-, M^-$ ) are similar to Eqs. (4.3), (4.4), (4.5), (4.6), (4.7), (4.8). The PDEs for subpopulation  $\text{Ph}^+$  (leukemia cells) ( $A^+, A^{*+}, P^+, M^+$ ) are similar to Eqs. (4.3), (4.4), (4.7), (4.8), while for  $\text{Ph}^+(\Omega^+, \Omega^{*+})$  subpopulation PDEs are modified as described in [17].

### Numerical Solution of Model III

Roeder et al. [25] conducted numerical studies of CML genesis from one leukemia stem cell. The transition from one leukemia cell to a BCR-ABL ratio of over 99 simulating the dynamics for up to 15 years. Such a long time simulation with a PDE model is challenging for traditional methods (e.g., finite difference, finite volume). To utilize the ability of wavelets for identification and isolation of localized structures, we solve PDEs arising from the model as discussed in previous subsection using a wavelet adaptive computational approach [26,27].

Figure 4 shows the number of mature  $\text{Ph}^-$  and mature  $\text{Ph}^+$  cells plotted against time. We observe from Fig. 4a that the number of nonleukemia cells decreases with time. Moreover, the number of leukemia affected cells increases in a leukemia patient in Fig. 4b. The corresponding grid for the simulation of nonleukemia and leukemia affected cells is also plotted in Fig. 4. When there is a sharp change in the  $\text{Ph}^-$  and  $\text{Ph}^+$  cells, the solution is automatically obtained using a finer mesh, while it is obtained using coarser mesh for the remaining part.

The coarser/finer mesh is automatically obtained depending on the behavior of cells which ensures the automatic adaptive feature of this approach.

## Concluding Remarks

The novelty of this work is in the mathematical results which indicate that the transient information about all the models of granulocytopoiesis can be predicted accurately by looking at the derived closed form solutions and numerical solution. These results serve not only to suggest a new direction for cancer research, but also to illustrate the need for understanding the transient development process of granulocytopoiesis against the dynamics of different treatments ([28] and [16]).

## References

1. Cronkite, E.P., Vincent, P.C.: Granulocytopoiesis. In: Stohman, F. (ed.) Hemopoietic Cellular Proliferation. Grune and Stratton, New York (1970)
2. Maloney, M., Patt, H.M.: Granulocyte transit from bone marrow to blood. *Blood* **31**, 195–201 (1968)
3. Ahmed, E., Hegazi, A.S., Elgazzar, A.S.: On difference equations motivated by modelling the heart. *Nonlinear Dyn.* **46**, 49–60 (2006)
4. Izzo, G., Vecchio, A.: A discrete time version for models of population dynamics in the presence of an infection. *J. Comput. Appl. Math.* **210**, 210–221 (2007)
5. Fokas, A.S., Keller, J.B., Clarkson, B.D.: Mathematical model of granulocytopoiesis and chronic myelogenous leukemia. *Cancer Res.* **51**, 2084–2091 (1991)
6. Cronkite, E.P., Vincent, P.C.: Granulocytopoiesis. *Ser. Haematol.* **2**, 3–43 (1969)
7. Rubinow, S.I.: A simple model of steady state differentiating cell system. *J. Cell Biol.* **43**, 32–39 (1969)
8. Rubinow, S.I., Lebowitz, J.L.: A mathematical model of neutrophil production and control in normal man. *J. Math. Biol.* **1**, 187–225 (1975)
9. Whittaker, J.A.: Leukemia. Blackwell Scientific Publisher, Oxford (1968)
10. Druker, B.J., Lydon, N.B.: Lessons learned from the development of an abl tyrosine kinase inhibitor for chronic myelogenous leukemia. *J. Clin. Investig.* **105**, 3–7 (2000)
11. Campbell, J.D., Cook, G., Holyoake, T.L.: Evolution of bone marrow transplantation—the original immunotherapy. *Trends Immunol.* **22**, 88–92 (2001)
12. Wheldon, T.E., Krik, J., Finlay, H.M.: Cyclical granulopoiesis in chronic granulocytic leukemia: a simulation study. *Blood* **43**, 379–225 (1974)
13. Loeffler, M., Wichmann, H.E.: A comprehensive mathematical model of stem cell proliferation which reproduces most of the published experimental results. *Cell Tissue Kinet.* **13**, 543–561 (1980)
14. Neiman, B.: A Mathematical Model of Chronic Myelogenous Leukemia. Oxford University, Oxford (2000)
15. Moore, H., Li, N.K.: A mathematical model for chronic myelogenous leukemia (CML) and T cell interaction. *J. Theory. Biol.* **225**, 513–523 (2004)
16. Kim, P.S., Lee, P.P., Levy, D.: Modelling imatinib-treated chronic myelogenous leukemia: reducing the complexity of agent-based models. *Bull. Math. Biol.* **70**, 728–744 (2008)
17. Kim, P.S., Lee, P.P., Levy, D.: A PDE model for imatinib-treated chronic myelogenous leukemia. *Bull. Math. Biol.* **70**, 1994–2016 (2008)
18. Liandrat, J., Tchamitchian, P.: Resolution of the 1d Regularized Burgers Equation Using a Spatial Wavelet Approximation. Technical Report , pp. 90–83, ICASE, (1990)
19. Vasilyev, O.V., Bowman, C.: Second generation wavelet collocation method for the solution of partial differential equations. *J. Comput. Phys.* **165**, 660–693 (2000)
20. Mehra, M., Kevlahan, N.K.-R.: An adaptive wavelet collocation method for the solution of partial differential equations on the sphere. *J. Comput. Phys.* **227**, 5610–5632 (2008)
21. Aldroubi, A., Unser, M.: Wavelets in Medicine and Biology. CRC press, Boca Raton (1996)
22. Mallik, R.K.: Solutions of linear difference equations with variable coefficients. *J. Math. Anal. Appl.* **222**, 79–91 (1998)
23. Mallik, R.K.: On the solution of a linear homogeneous difference equation with variable coefficients. *Siam J. Math. Anal.* **31**, 375–385 (2000)



24. Blumenson, L.E.: A comprehensive modelling procedure for the human granulopoietic system: over-all view and summary of the data. *Blood* **42**, 303–312 (1973)
25. Roeder, I., et al.: Dynamic modeling of imatinib treated cml: functional insights and clinical implications. *Nat. Med.* **12**, 1181–1184 (2006)
26. Jameson, L.: On the Wavelet-Optimized Finite Difference Method. ICASE CR-191601 (1994)
27. Kumar, V., Mehra, M.: Wavelet optimized finite difference method using interpolating wavelets for self-adjoint singularly perturbed problems. *J. Comput. Appl. Math.* **230**, 803–812 (2009)
28. Michor, F., Hughes, T.P., Iwasa, Y., Branford, S., Shah, N.P.: Dynamics of chronic myeloid leukemia. *Nature* **435**, 1267–1270 (2005)